J Wood Sci (2004) 50:28–34
DOI 10.1007/s10086-003-0527-9

ORIGINAL ARTICLE

Jean-Philippe Costes · Pak Lim Ko · Tony Ji
Cyrille Decès-Petit · Yusuf Altintas

Orthogonal cutting mechanics of maple: modeling a solid wood-cutting process

Received: August 28, 2002 / Accepted: February 14, 2003

Abstract The experimental results of orthogonal cutting of maple and the modeling of the cutting mechanics are presented. The tool cutting forces were measured for different feed rates. A set of equations relating the tangential and feed forces to the tool edge width and feed rate (chip thickness) to calculate the chip and edge cutting force coefficients was developed. Then the chip force and edge force coefficients were calculated from experimentally obtained cutting forces and were plotted in a polar-coordinate system with respect to the fiber orientation of the maple disk. The polar-coordinate presentation of the cutting force results and the calculated cutting force coefficients provides an excellent visual appreciation of the relation between the cutting forces and the wood fiber orientation. Chips were also collected from various sectors of the wood disk. This analysis further identified the effects of fiber orientation and cutting forces on the types of chip formed and hence the cutting mechanics involved. By applying the calculated cutting coefficients for each tool orientation (in respect to the grain) it is possible to predict the feed and tangential forces for any feed rates. There is good agreement between the predicted and measured cutting forces.

Key words Orthogonal cutting · Fiber orientation · Cutting force · Wood chip

Introduction

During the 1950s Kivimaa,[1] Franz,[2] and McKenzie[3] studied the mechanics of orthogonal wood cutting and, in particular, the relation between the tool forces and that of the rake angle used and the resultant chip thickness. Their publications remain the major source of references. McKenzie described three basic types of orthogonal cutting of green wood using two numbers representing (1) the angle between the cutting edge of the tool and the cellular grain direction and (2) the angle between the direction of cutting and the grain direction. The numbers are either 90 for normal or 0 for parallel. McKenzie and Franz further described the various types of chip that would be expected under different tool geometry and cutting conditions. One of the objectives of these past studies and the present one is to develop models to predict the cutting forces.

There have been attempts to use the finite element technique to develop models in wood cutting studies.[4] However, wood being an anisotropic material presents a significant challenge in modeling the influence of the grain direction and the changes in material properties along the cutting direction. Although it is possible to predict the direction of failure in solid wood, it is difficult to predict the cutting forces owing to the unpredictable variations in material properties.

In Holmberg's finite element model, he superimposed several layers of isotropic material with incremental mechanical properties to simulate the orthotropic structure of wood. However, the simulated cutting speed used in the model was much lower than that used in a realistic wood cutting process. A medium density fiberboard (MDF), which is closer to an isotropic material, can be expected to give more consistent results and is therefore more suitable for studying the fundamentals of wood cutting. For example, McKenzie et al.[5] established a predictive model of cutting forces and surface quality in MDF that may be assumed to have a uniform material property on the surface, although its hardness and density decrease rapidly toward the core. At around the same time, Dippon et al.[6] presented an orthogonal cutting test strategy to extract average friction and normal forces acting on the tool. They developed a set of constants in terms of tool rake angle, layer depth (micro-hardness), and feed rate for cutting MDF. These orthogonal cutting constants were trans-

J-P. Costes · T. Ji · Y. Altintas
Department of Mechanical Engineering, University of British Columbia, Vancouver, BC, Canada

P.L. Ko · C. Decès-Petit (✉)
National Research Council Canada, 3250 East Mall, Vancouver, BC, V5T 1W5, Canada
Tel. +1-604-221-3125; Fax +1-604-221-3088
e-mail: cyrille.deces-petit@nrc.ca

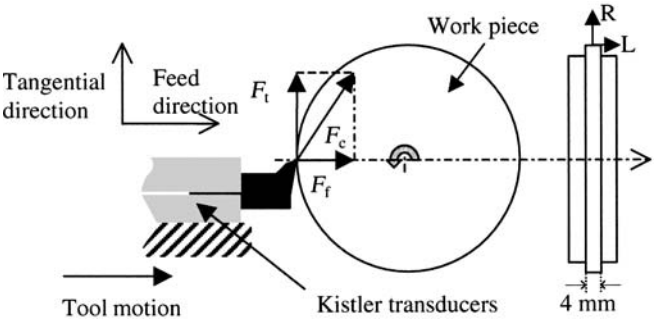

Fig. 1. Experimental setup for plunge turning

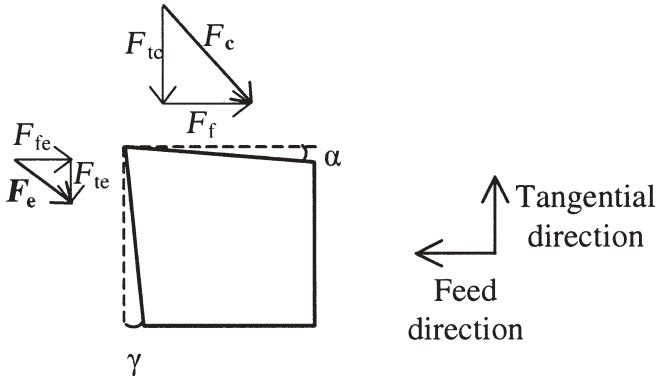

Fig. 2. Free-body force diagrams of the tool during orthogonal cutting

formed into an oblique plane of cut allowing accurate prediction of cutting forces for routers having an arbitrary geometry.[7] In their studies, the friction and normal load on the cutting tool were considered point loads. Ko et al.[8] carried out an extensive parametric study in orthogonal machining MDF, in which they described a technique to present the measured forces in polar coordinates. Earlier, Ko et al.[9] used the technique to superimpose the polar-force diagram on the disk surfaces of some green wood species to obtain a correlation between the forces and the wood grain directions. This same experimental process has been employed in the present study to establish a relation between the cutting forces and the tool direction/grain relative orientation for machining maple.

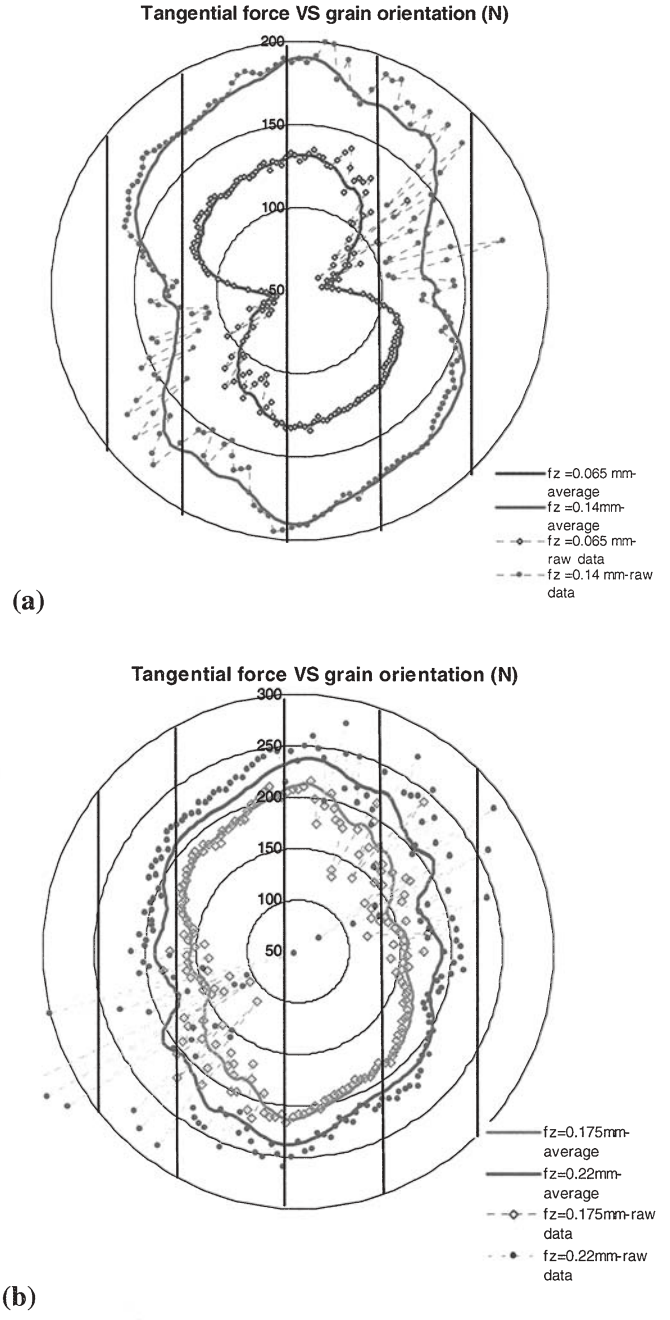

Fig. 3. Tangential force versus grain orientation for (**a**) feed rates 0.065 and 0.14 mm·rev^{-1} and (**b**) feed rates 0.175 and 0.22 mm·rev^{-1}. The vertical axis corresponds to the fibers' orientation

Materials and methods

Experimental setup

A Turnmaster TRL1340 lathe was used for the cutting experiment. Cutting forces were monitored and recorded by a dynamometer equipped with two Kistler triaxial piezoelectrical force transducers, which were built into the tool holder assembly, and a data acquisition board with an acquisition frequency of 300 Hz. Four feed rates (0.06, 0.15, 0.19, and 0.24 mm·rev^{-1}) were tested. The spindle, which held the maple disk, was run at 100 rpm. The tool has a rake angle of 10° and a clearance angle of 12° with a width of 6.5 mm. Maple disks were cut from British Columbian (Canada) grown bigleaf maple (*Acer macrophyllum*). The density at 12% moisture content was 560 kg·m^{-3}. A 4-mm ring was premachined to ensure a continuous width of cut.

Mathematical analysis of cutting forces

For orthogonal cutting, two fundamental cutting forces – the tangential force F_t, which is parallel to the direction of the cutting speed, and the feed force F_f, which is perpen-

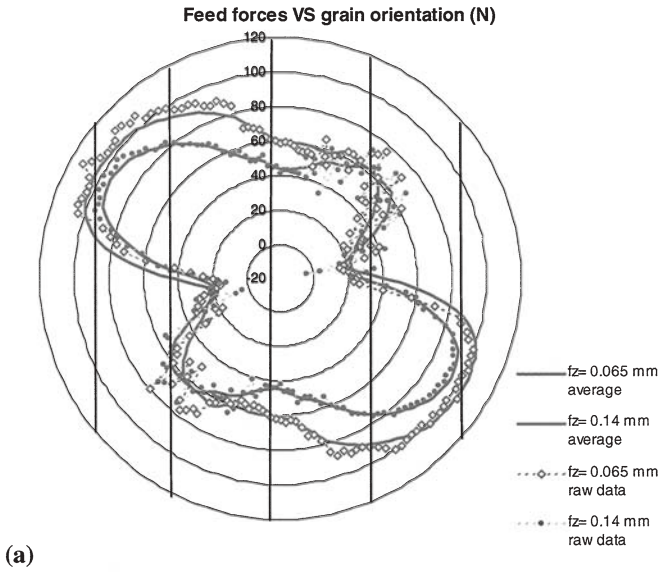

(a)

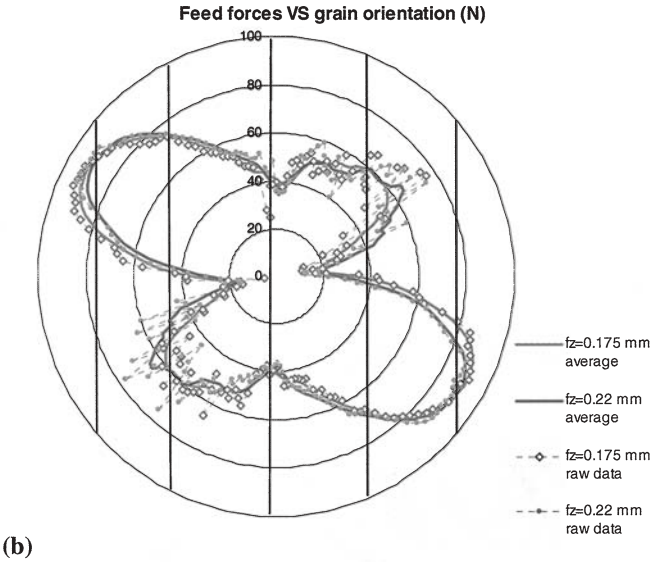

(b)

Fig. 4. Feed force versus grain orientation for (**a**) feed rates 0.065 and 0.14 mm·rev^{-1} and (**b**) feed rates 0.175 and 0.22 mm·rev^{-1}. The vertical axis corresponds to the fibers' orientation

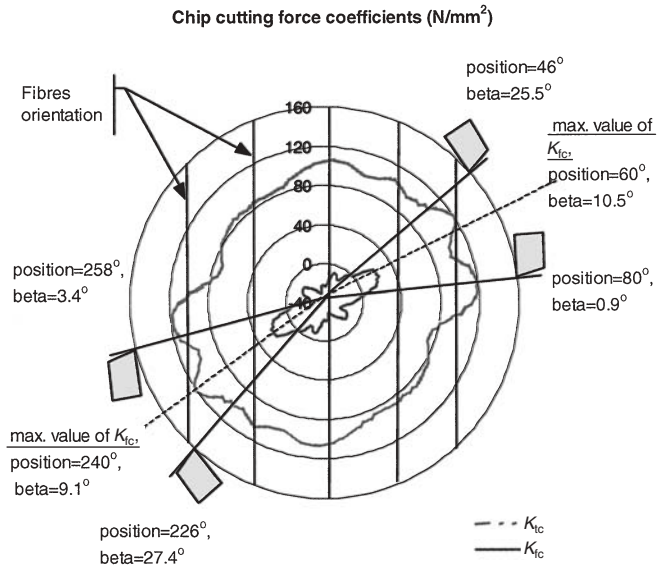

Fig. 5. Chip-cutting force coefficients in the feed K_{fc} and tangential K_{tc} directions versus grain orientation showing the maximum orientation (*dashed line*) and the visually drawn transitional boundaries (*solid lines*)

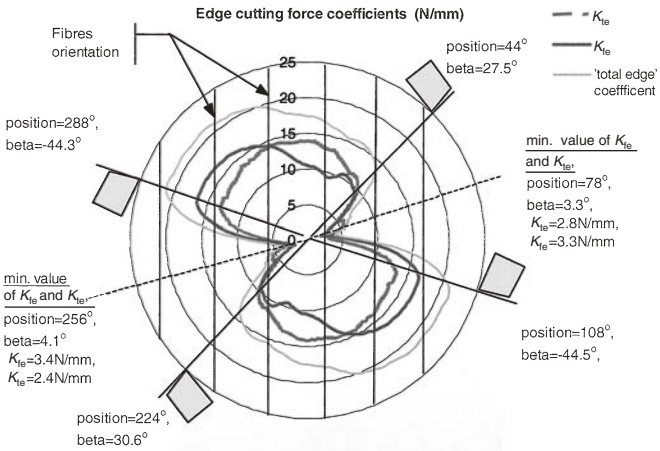

Fig. 6. Edge-cutting coefficients in feed K_{fe} and tangential K_{te} directions versus grain orientation showing the minimum orientation (*dashed line*) and the visually drawn transitional boundaries (*solid lines*). β is the value of the angle between total force and fibers direction

dicular to the direction of the cutting speed (Fig. 1) – are considered.[10] Each of these two cutting forces can be divided into two parts: one as an edge force component, which acts between the flank face and the wood surface, and the other a chip force component, which acts between the rake face and the chip. The components on the flank face can be summed to form the edge force F_e; similarly, the components on the rake face can be summed to form the chip force F_c (Fig. 2). For a sharp-edged tool we may assume that F_e is applied at the edge as a line force, and F_c is applied on the rake face. If the chip force is assumed to be proportional to the uncut chip area bh, and the edge force is related to the width of cut b, only then can equations for the tangential and feed forces be constructed.

$$F_t = F_{tc} + F_{te} = K_{tc}bh + K_{te}b \tag{1}$$

$$F_f = F_{fc} + F_{fe} = K_{fc}bh + K_{fe}b$$

where h denotes the uncut chip thickness (or feed rate during orthogonal cutting), b is the width of the cut, and (K_{tc}, K_{fc}) and (K_{te}, K_{fe}) are the cutting coefficients corresponding to the chip and edge forces, respectively.

For zero uncut chip thickness ($h = 0$), both F_{tc} and F_{fc} equal zero. Thus, Eq. (1) becomes

$$F_{te} = F_t \quad \text{and} \quad F_{fe} = F_f \quad \text{for} \quad h = 0 \tag{2}$$

The cutting coefficients can be calculated from measured tangential F_t and feed F_f forces. A series of orthogonal cutting tests would be conducted at incremental feed rates, and the two orthogonal cutting forces would be measured.

By extrapolating the measured data at zero uncut chip thickness (i.e., $h = 0$), the edge force constants (K_{te}, K_{fe}) could be evaluated. After subtracting the edge force from each measurement, the cutting coefficients (K_{tc}, K_{fc}) could be evaluated as well.

Results

Measured cutting forces

The conventions used for the tool forces in this study are as follows: Positive tangential force acts opposite to the direction of the tool motion, and positive feed force acts to push the tool away from the wood disk.

In most cases, the force signal was averaged over a number of disk cycles and then plotted against the cut distance at regular intervals. Force data can be plotted in either rectilinear coordinates or polar coordinates. In the latter format, the polar-force diagram using a reference marker on the disk during data acquisition can be superimposed on the surface of the machined disk, providing a convenient way to display the correlation between the cutting force and the grain structure during solid wood machining.[8,9]

The cutting forces are displayed in the polar-coordinate format in Figs. 3 and 4. The orientation of the individual force vector coincides with the corresponding location of the tool–disk contact location during cutting. For each feed rate two sets of measured force data were presented. One set of force data, which displays many spikes of force peaks, was obtained by simply averaging the force data from several cut cycles. The other set of force data, which appears to be smooth without the spikes, was obtained by a moving averaging technique to filter out the high-frequency peaks. Furthermore, it is assumed that the disk has an axial symmetrical property, and the measured forces from the diametrically opposite locations were averaged. In these figures, The vertical lines in Figs. 3 and 4 represent the grain orientation on the disk, and the circles are incremental force grids in newtons.

Calculated cutting force coefficients

The cutting force coefficients were calculated by applying the measured forces (moving averaged) to Eqs. (1) and (2). The results are shown in Figs. 5 and 6.

From Figs. 3–6, one notes the axial symmetry (relative to the disk center) of the measured forces and the calculated coefficients because of the assumption of axial symmetry

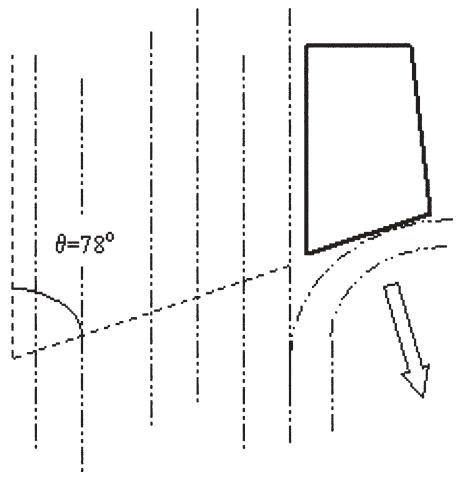

Fig. 7. For a 78° tool position, the clearance face is parallel to the fibers; the measured forces are minimum

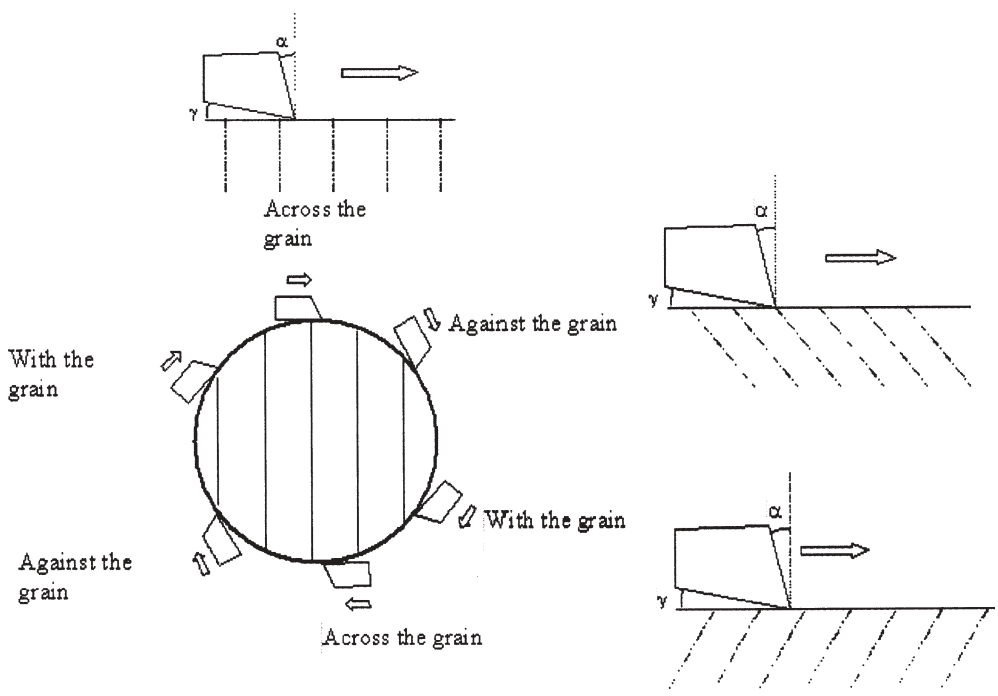

Fig. 8. Evolution of the cutting process during one disk revolution

applied to the force data. For most tool positions (relative to the grain orientation), the chip coefficient in the feed direction K_{fc} appears to be negative (around $-20\,N{\cdot}mm^{-2}$). In other words, the feed force tends to decrease with increasing feed rates for most of the tool positions with the exception of 46°–80°, where the K_{fc} values are positive. The chip coefficient in the tangential direction (K_{tc}) is positive all around the disk with a fairly steady distribution (about $80\,N{\cdot}mm^{-2}$). Overall, the K_{tc} plots appear to be smooth, with the exception around the sector 46°–80° where the K_{tc} values appear to be spiky with significant deviations. This K_{tc} sector coincides with the sector where K_{fc} is positive.

Effect of tool location and fiber orientation on cutting force coefficients

Figure 6 shows that from around 95° (shoulder at 108°) to 238° (shoulder at 224°) both K_{te} and K_{fe} have high values 10–$16\,N{\cdot}mm^{-1}$. Whereas K_{fe} drops from $16\,N{\cdot}mm^{-1}$ in the first half of this sector to just below $10\,N{\cdot}mm^{-1}$, K_{te} increases from about $12\,N{\cdot}mm^{-1}$ to $15\,N{\cdot}mm^{-1}$. The transition appears to occur when the tool is going through the 0° (or 180°) angle position, that is, when machining changes from with-the-grain direction to against-the-grain direction. Actually, when K_{fe} is decreasing, K_{te} is increasing in such a way that the vector sum of the edge coefficient ($\sqrt{(K_{te})^2 + (K_{fe})^2}$) remains fairly constant in the range between 95° (shoulder at 108°) to 238° (shoulder at 224°). At 44°–78° the K_{te} and K_{fe} values decrease sharply to their respective minimum values around $5.5\,N{\cdot}mm^{-1}$ and $1.7\,N{\cdot}mm^{-1}$. Also at this point the total force vector, calculated from F_t and F_f components, is almost aligned with the fibers' orientation, which is the angle β between the calculated total force direction and the fibre orientation, is about 0°. Then the edge components start to increase again, reaching a maximum at about 108°. One may speculate that between 44° and 108°, a splitting process occurs between the fibers, which results in a lower resultant force. Furthermore, the changes in the forces and coefficient values may be explained by the tool geometry; for a 78° tool position, a clearance angle of 12° would have the clearance face parallel to the grain direction. In this instance, the clearance face and the edge are

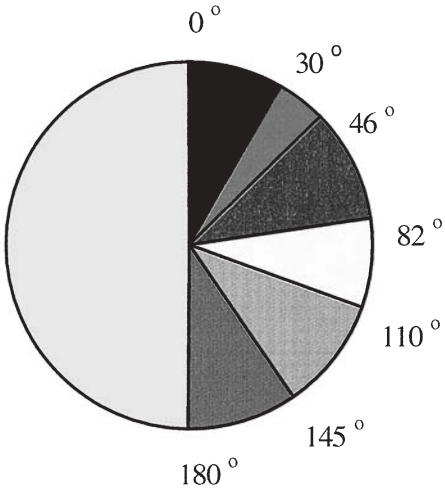

Fig. 9. Maple disk pattern before cutting tests for chip analysis

Fig. 10. Chip shape versus tool position and cutting pattern

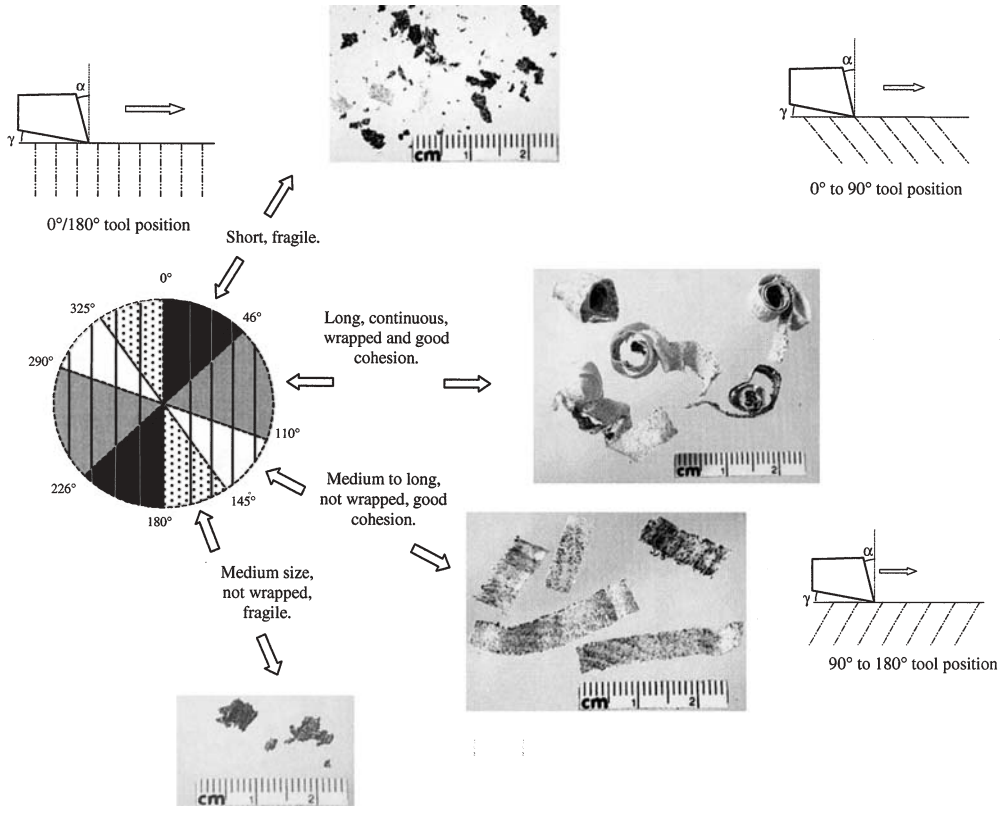

Table 1. Analysis of chip shape versus tool/fibers relative location for two sets of experiments

Tool/fiber relative angle (°)	0.15 mm/rev					0.24 mm/rev				
	General shape	Continuous	Cohesion	Length (mm)	Wrapped	General shape	Continuous	Cohesion	Length (mm)	Wrapped
0–30	Short chip, fragile	No	No	1–2	No	Short chip, fragile	Sometimes	Not good	<5	No
30–46	Short chip, fragile	No	No	1–2	No	Short chip, fragile	No	No	1–2	No
46–82	Long, continuous, wrapped	Yes	Good	>10	Yes	Long, continuous, wrapped	Yes	Good	>10	Yes
82–110	Long, continuous wrapped	Yes	Good	>10	Yes	Long, continuous wrapped	Yes	Good	>10	Yes
110–145	Long, continuous	Yes	Good	>10	No	Long, continuous	Yes	Good	>10	No
145–180	Medium length, continuous, fragile	Yes	Not good	~5	No	Medium length, continuous, fragile	Yes	Not good	~5	No

"sliding" along the fibers and into the interfiber space, as illustrated in Fig. 7. This may lead to low cutting forces, as the fibers are not severed but simply separated from each other. Recall that the 78° tool position corresponds to the minimum edge force coefficients (K_{te}, K_{fe}) and minimum cutting forces (F_t, F_f). From the 78° tool position, as the cutting process changes from "against-the-grain" to "with-the-grain," the measured force results become fairly consistent, with little deviation from its mean value. On the other hand, when cutting between 12° and 78°, the "against-the-grain" cutting process may explain the rugged force values obtained. The different patterns of the cutting process encountered during one complete revolution of the disc specimen are summarized in Fig. 8.

Chip analysis

To facilitate chip examination after cutting, two maple disks were painted with different colored sectors, as shown in Fig. 9. The sector's angles were chosen in accordance with the results presented in Figs. 5 and 6. Two sets of cutting tests with feed rates at 0.15 and 0.24 mm·rev^{-1} were carried out.

Chips were collected for analysis after about 15 cut-revolutions. The analysis focused on the size and length of the chips and whether the chips were rolled or flat. The results are presented in Table 1.

Figure 10 summarizes the various chip characteristics on a cut-disk surface to illustrate the relation between the tool–fiber orientation and the resultant chip formation. The results show that long, continuous chips are likely the result of splitting when the tool is cutting close to the grain orientation. When the rake face is orthogonal to the grain, the chips are curled.

Application of the calculated cutting force coefficients

A cutting test using the same tool and similar cutting conditions but with a feed rate at 0.275 mm·rev^{-1} was carried out to evaluate the effectiveness of the calculated cutting force coefficients. The cutting forces F_t and F_f were measured and plotted in polar coordinates, as shown in Fig. 11. Next, simulated F_t and F_f plots using the coefficients (K_{tc}, K_{fc}) and (K_{te}, K_{fe}) generated earlier for disk angles 0°–180° and Eq. (1) were developed and superimposed on the respective charts in Fig. 11.

The results in Fig. 11 show that the measured and predicted cutting forces are in good agreement. The standard deviation between the measured and predicted forces F_t and F_f along the polar curves are about 6% and 14%, respectively. The gap between the predicted and measured forces appears to be the same for F_t and F_f. Because the feed force values are about one-third the tangential force values, the absolute values of error are about the same for both cutting forces. It appears that the largest gap between the measurement and the prediction occurs when cutting was performed across the grain (0° and 180° position). It has been noted earlier that cutting across the grain generates short, fragile chips. The cutting forces in this sector may not

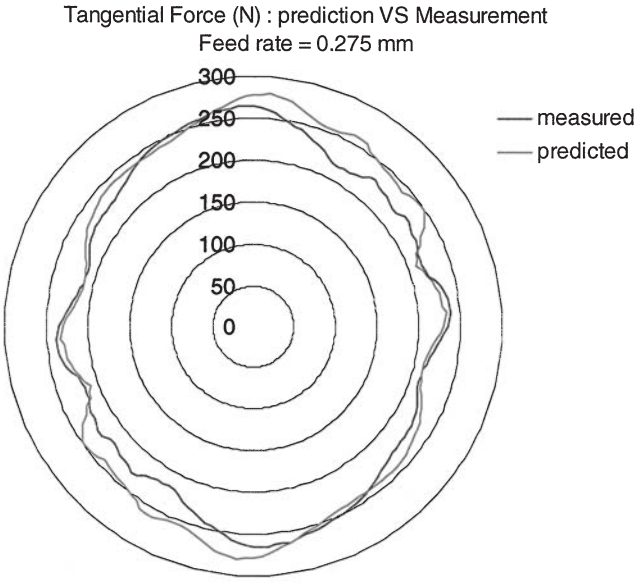

(a) Measured and predicted tangential forces

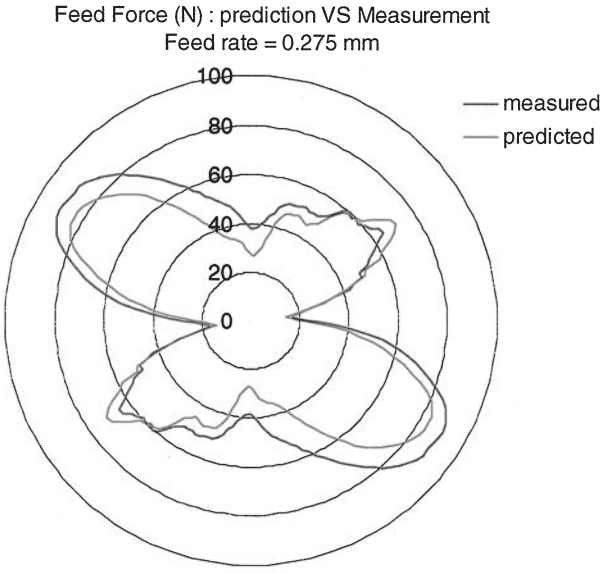

(b) Measured and predicted feed forces

Fig. 11. Comparison of measured and predicted cutting forces for one revolution of cut

be as consistent as in other sectors, such as when cutting with the grain, resulting in a less accurate set of force coefficients around this sector.

Conclusions

The polar-coordinate presentation of the cutting force results provides an excellent visual appreciation of the relation between the cutting forces and subsequently the cutting force coefficients with wood fiber orientation. Subsequent analysis of chips collected from various sectors of the wood disk further identified the effects of fiber orientation and cutting forces on the types of chip formed and hence the cutting mechanics involved.

Applying the calculated cutting coefficients K_{te}, K_{fe} and K_{tc}, K_{fc} for each tool motion orientation (with respect to the grain), it is possible to predict the feed and tangential forces for any feed rates and tool geometry (so long as the rake and clearance angles are kept constant). There is good agreement between the predicted and measured cutting forces. This model could be further used for predicting cutting forces for milling solid wood where the angle of the edge motion and the grain varies along the edge path. Similar studies should be carried out for other wood species to build a database of cutting coefficients that would be useful for cutting process simulation.

References

1. Kivimaa E (1950) Cutting force in wood working. PhD thesis, Finland State Institute for Technical Research
2. Franz NC (1958) Analysis of the wood cutting process. Engineering Research Institute, University of Michigan Press, Ann Arbor
3. McKenzie WM (1961) Fundamental analysis of the wood cutting process. PhD thesis, University of Michigan, Department of Wood Technology
4. Holmberg S (1998) A numerical and experimental study of initial defibration of wood. Report TVSM 1010. Lund University/Lund Institute of Technology, Sweden, p 203
5. McKenzie WM, Ko PL, Cvitkovic R, Ringler T (1999) Towards a model predicting cutting forces and surface quality in routing layered boards. Presented at the 14th international wood machining seminar, France, pp 489–497
6. Dippon J, Ren H, Ben Amara F, Altintas Y (2000) Orthogonal cutting mechanics of medium density fiberboards. Forest Prod J 50:25–30
7. Engin S, Altintas Y, Ben Amara F (2000) Mechanics of routing medium density fiberboard. Forest Prod J 50:65–69
8. Ko PL, McKenzie W, Cvitkovic R, Robertson MF (1999) Parametric studies in orthogonal machining MDF. Presented at the 14th international wood machining seminar, France, pp 1–12
9. Ko PL, Hawthorne HW, Andiappan J (1998) Tribology in secondary wood machining. ASTM special publication: STP 1362 wear process in manufacturing, pp 101–120
10. Altintas Y (2000) Manufacturing automation: metal cutting mechanics, machine tool vibrations, and CNC design. Cambridge University Press, New York

The publication of this article was made possible by an Emachu Research Fund. The authors are grateful for the fund.